Laminar Flow and Heat Transfer of Impinging Slot Jet onto Sinusoidal Target Surface

H. H. Sarhan
Department of Mechanical Power Engineering – Faculty of Engineering
Port Said University – Port Said - EGYPT

Abstract

An investigation of the laminar flow field and heat transfer characteristics of a slot jet impinging onto a sinusoidal target surface is carried out numerically in this study. Air is used as working fluid with constant properties with uniform velocity and temperature profiles at the jet exit. According to finite volume technique, the partial differential equations are transformed to associated sets of linear algebric equations. The systems of algebraic equations are solved using Gauss-Siedel iteration method. A computer program in FORTRAN is developed to perform the numerical solution of these sets. The derived proposed model is used to study the effect of problem parameters: Reynolds number (Re = 50 - 600), dimensionless slot jet width (B = 0.5 – 1.0), dimensionless surface wave amplitude (A = 0.0 - 0.5) and dimensionless surface wave length (S = 1.0 – 5.0). The flow field, local Nusselt number and, in turn, average Nusselt at the impinging target sinusoidal surface are evaluated at different values of the problem parameters.

1. Introduction

Jet impingement is an important subject in engineering that it provides rapid cooling, drying, heating or mixing. Numerous applications are found as tempering of glass, drying of textiles or paper, internal combustion engines, freezing of tissue, cooling of metal sheets, microelectronic components, cooling of electronic equipment, cutting, and turbine blades. The past studies in literature included the fundamental of jets and listed applications [1-3]. Applications are separated in two categories: heating/cooling configurations either at a constant wall temperature (quench cooling) or at a uniform wall heat flux (electronic components cooling). While the impinging surfaces are separated in two categories: linear (horizontal, vertical and oblique) and nonlinear (cavity, cylinder, wavy and sphere).

Considering linear impinging surface, Chattopadhayay and Saha [4] used the LES to investigate the turbulent flow and heat transfer due to a single slot-jet impingement on a moving hot isothermal plate. Only one jet exit Reynolds number of 5800 and only one normalized jet to target spacing of 8.0 for normalized plate velocities of 0.0 to 2.0 are examined. The study is mainly concentrated on the details of the flow structure and velocity profiles and distribution of turbulent stresses. Isman et al. [5] numerically investigated flow and heat transfer characteristics for the impingements of the single and double free jets on a surface with constant heat flux. Steady, incompressible, two-dimensional and turbulent flow is considered. Lee et al. [6] numerically investigated the fluid flow and heat transfer in confined impinging slot jet in the low Reynolds number region for different channel heights. A big impact of the unsteadiness due to the pressure coefficient, skin friction coefficient and Nu number in the unsteady region is found. Dagtekin and Oztop [7] studied heat transfer due to double impinging vertical slot jets onto an isothermal wall is investigated numerically for laminar flow regime. The effect of the jet Reynolds number, the jet isothermal bottom wall spacing, and the distance between two jets on heat transfer and flow field is examined. Convective heat transfer from a moving isothermal hot plate due to confined slot-jet impingement is investigated numerically by Sharif and Banerjee [8]. Steady and two-dimensional turbulent flow is considered. The rectangular flow geometry consists of a confining adiabatic wall placed parallel to the moving impingement surface with the slot-jet located in the middle of the confining wall. The k-ε turbulence model with enhanced wall treatment is used for the turbulence computations. The jet exit Reynolds number, ranging from 5000 to 20,000, the normalized plate velocity, ranging from 0.0 to 2.0, and the normalized distance of separation between the impingement plate and the jet exit, ranging from 6.0 to 8.0 are used as problem parameters. Ibuki [9] et al. investigated experimentally the heat transfer

characteristics of a planar free water jet normally or obliquely impinging onto a flat substrate. Reynolds number, impingement angles between the vertical planar jet and the inclined solid surface are considered as problem parameters with constant heat flux at the solid surface. The stagnation Nusselt numbers are compared to the predictions of several correlations proposed by other researchers. In oblique collisions, the profiles of the local Nusselt numbers are found to be asymmetric. The thermal characteristics of confined and unconfined impinging jets are compared by Choo and Kim [10]. The results showed that, the thermal performance of the confined jet are similar to that of the unconfined jet under a fixed pumping power condition, while the thermal performance of the confined jet are 20–30% lower than that of the unconfined jet under a fixed flow rate condition. Generalized correlations for the stagnation and average Nusselt numbers for both confined and unconfined impinging jets are presented as a function of the dimensionless pumping power and the Prandtl number. Slot-jet impingement systems are recognized in their ability to control fluid flow for high energy transfer on the target surface by Na-pompet and Boonsupthip [11]. Considering the modified slot-jet impingement system with additional horizontal and vertical plates, the overall heat transfer over the target impinging surface is enhanced. Considering the horizontal plate height value, stronger effect on Nusselt number distribution profiles on the target surface is found than that of the distance from nozzle edge to vertical plate value. It is demonstrated that, a proper design of the plate position significantly enhanced the overall energy transfer on the target surface and improved the cooling rate of food model.

Considering nonlinear impinging surface, McDaniel and Webb [12] studied experimentally the heat transfer characteristics of circular cylinders exposed to slot jet impingement. Both contoured orifice and sharp-edged orifice jet configurations are investigated. It is concluded that, the slot jet yielded considerably higher average heat transfer from the cylinder when compared to the infinite parallel flow case on the basis of identical average velocity in the slot jet and infinite flow configurations. Chan et al. [13] examined the turbulent structure of a plane jet impinging on a convex semi-cylinder that lied on a flat surface. Measurements are showed that, the profiles of mean flow velocity in the wall jet are self-similar with respect to the nozzle-to-cylinder distance, whereas the intensity of velocity pulsations is shown to grow with this parameter. Gori and Bossi [14] made several experiments on cooling performance of slot air jet along the surface of electrically heated circular cylinders. Investigation is focused on the effects of diameter to slot height ratios parameter on the value of average Nusselt number. It is indicated that, the definition of Nusselt and Reynolds numbers based on cylinder diameter and slot height represented an important factor to analyze the study. The flow structure and heat transfer during impingement cooling of an obstacle in the form of spherical cavity with an axisymmetric jet flow is examined by Kanokjaruvijit and Martinez-Botas [15]. The surfaces modified with cavities are proved to be efficient design in cooling internal flow paths of gas-turbine blades with a system of impact jets. Shuja et al. [16] examined the effects of jet velocity at nozzle exit onto the flow structure in the region of the cavity and heat transfer rates from the cavity surface. An experimental study of flow characteristics and heat transfer for jet impingement cooling of obstacles in the form of single spherical cavities is reported by Terekhov et al. [17]. The distributions of flow velocities between the nozzle and the obstacle, and also the fields of pressure and heat-transfer coefficients inside the cavity are measured. Generally, at a value of depth the cavity, the large-scale toroidal vortex is generated and consequently influencing on the heat transfer. The cavity flow became unstable, exhibiting low-frequency pulsations of local heat fluxes. Numerical investigation of convective heat transfer process from concave cylindrical surface due to slot-jet impingement is performed by Sharif and Mothe [18]. The results indicated that, the jet-exit Reynolds number and the surface curvature is found to be significant effect on the heat transfer process. Celik [19] experimentally compared the cooling characteristics of roughened and smooth heated Surfaces subjected to co-axial impinging jet. The experiment is carried out for different Reynolds number and jet exit spacing. The average Nusselt number with coaxial jet impingement to the roughened surface is increased by up to 27 % comparing to the circular jet impingement. Also, the average Nusselt number is increased with roughened surface by up to 6 % over the whole surface area, comparing to the smooth surface. An investigation of the flow field and heat transfer characteristics of a slot turbulent jet impinging on a semi-circular concave surface with uniform heat flux is carried out numerically by Yang et al. [20]. The turbulent governing equations are solved by a control volume based finite-difference method with a power-law scheme and the well-known k–ε turbulence model and its associate wall function to describe the turbulent structure. In addition, a

body-fitted curvilinear coordinate system is employed to transform the physical domain into a computational domain. Varol et al. [21] performed a numerical investigation of two-dimensional slot impingement onto two heated cylinders with different diameters turbulent flow conditions. Jet Reynolds number, diameter ratio of cylinders and ratio of distance between cylinders to slot jet high are considered as problem parameters. Streamlines, isotherms, local and mean Nusselt numbers and drag coefficient are obtained. The results are compared with earlier experimental and numerical works and good agreement is obtained. The diameter ratios of cylinders are found to be a control element for heat and fluid flow.

The present work investigate numerically laminar flow and heat transfer of slot jet impingement onto sinusoidal surface with symmetrical exhaust ports in the confinement surface. The derived proposed model is used to study the effect of problem parameters: Reynolds number (Re = 50-600), dimensionless slot jet width (b/H = 0.5 – 1.0), dimensionless surface wave amplitude (a/H = 0.0 - 0.5) and dimensionless surface wave length (s/H = 1.0 – 5.0). The flow field, local Nusselt number and, in turn, average Nusselt at the impinging wall are evaluated at different values of the previously mentioned parameters considering air as working fluid.

2. Mathematical Formulation

A schematic diagram for the problem configuration is shown in Figure 1. Due to symmetry of configuration about the vertical y-axis, only the right half of the domain is considered. The jet exits through a horizontal slot of width (b) which, are placed symmetrically at the middle of the inlet surface of the domain while the rest of the surface is adiabatic..

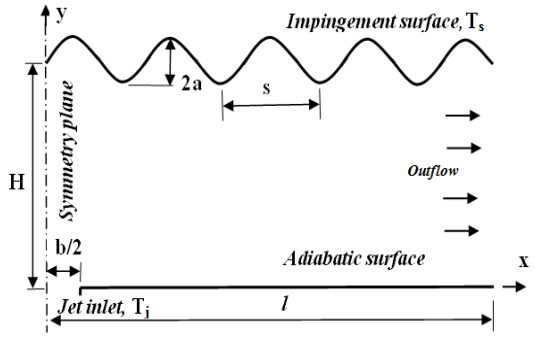

Figure 1. Schematic diagram of the flow domain considered in present study.

The length of the computational domain is l while the height is H, which signifies the separation distance between the jet exit and impingement sinusoidal surface

The length of the computational domain in the x-direction is approximately l = 120 b, which is quite longer, to ensure the traction-free boundary condition at the exit. Since the region of adverse pressure gradient (recirculation zone) is found to be long, the computational domain is extended long enough to attain a fully developed velocity profile at the exit. The initial jet temperature (T_j) and jet inlet velocity (v_j) are assumed to be uniform. The impingement surface is maintained at constant temperature isothermal (T_s).

The slot, in present study, is assumed to be large in the span-wise direction. Hence, the flow configuration is considered as a two-dimensional planar jet. Slot jets provide a larger impingement zone and lead to a uniform coolant rejection after impingement. To put the governing equations and their boundary and initial conditions in dimensionless form, one introduces the following dimensionless independent and dependent variables as follow:

$$X=\frac{x}{H},\ Y=\frac{y}{H},\ B=\frac{b}{H},\ A=\frac{a}{H},\ S=\frac{s}{H},\ L=\frac{l}{H}$$

$$U=\frac{u}{v_j},\ V=\frac{v}{v_j},\ P=\frac{p}{\rho v_j^2}\ \text{and}\ \theta=\frac{(T-T_\infty)}{(T_j-T_\infty)} \quad (1)$$

Where, P, θ, U and V are the dimensionless pressure, dimensionless temperature, the dimensionless velocity components in the x and y directions respectively. Considering the foregoing defined dimensionless variables, the dimensionless mass, momentum, and energy conservation equations for steady, two-dimensional, laminar, incompressible flow with constant fluid properties are written as:

$$\frac{\partial U}{\partial X}+\frac{\partial V}{\partial Y}=0 \quad (2)$$

$$U.\frac{\partial U}{\partial X}+V\frac{\partial U}{\partial Y}=-\frac{\partial P}{\partial X}+\frac{1}{Re}\left(\frac{\partial^2 U}{\partial X^2}+\frac{\partial^2 U}{\partial Y^2}\right) \quad (3)$$

$$U.\frac{\partial V}{\partial X}+V\frac{\partial V}{\partial Y}=-\frac{\partial P}{\partial Y}+\frac{1}{Re}\left(\frac{\partial^2 V}{\partial X^2}+\frac{\partial^2 V}{\partial Y^2}\right) \quad (4)$$

$$U\frac{\partial \theta}{\partial X}+V\frac{\partial \theta}{\partial Y}=\frac{1}{Re\cdot Pr}\left(\frac{\partial^2 \theta}{\partial X^2}+\frac{\partial^2 \theta}{\partial Y^2}\right) \quad (5)$$

Knowing that, gravity, viscous dissipation and radiation effects are neglected. Where, Pr and Re are Prandtl and Reynolds numbers respectively, which are defined as:

$$Pr=\frac{\nu}{\alpha}\ \text{and}\ Re=\frac{v_j\, b}{\nu} \quad (6)$$

Where, ν and α are the kinematics viscosity and thermal diffusivity of the fluid respectively. The dimensionless equations (2-5) must satisfy the following boundary conditions:

At jet exit: $Y= 0, 0 < X \leq 0.5$

$U = 0, V = 1, P = 0$ and $\theta = 1$

At adiabatic surface: $Y = 0, 0.5 < X \leq L$

$U = V = 0, P = 0$ and $\frac{\partial \theta}{\partial Y} = 0$

At flow outlet: $0 < Y < 1, X = L$ (7)

$\frac{\partial U}{\partial X} = 0, \quad \frac{\partial P}{\partial X} = 0$ and $\frac{\partial \theta}{\partial X} = 0$

At target surface: $Y = 1, 0 < X \leq L$

$U = 0, V = 0, P = 0$ and $\theta = \theta s$

At symmetry plane: $0 \leq Y \leq 1, X = 0$

$U = 0, \quad \frac{\partial V}{\partial Y} = 0, \quad \frac{\partial P}{\partial X} = 0$ and $\frac{\partial \theta}{\partial X} = 0$

Both, the local and average Nusselt number (Nub, Nu) are calculated as;

$$Nu_b = \left(\frac{B}{\theta_s - 1}\right)\left(\frac{\partial \theta}{\partial Y}\right)_{@\,Sinusoidal surface} \quad (8)$$

$$Nu = \frac{1}{L}\int_0^L Nu_b \, dX \quad (9)$$

3. Numerical Procedure

The geometric boundaries and physical conditions are assumed to be symmetric about the centreline of the jet; therefore, only half the physical domain is considered in numerical models. The governing equations are solved numerically using finite volume technique. According to this technique, partial differential equations which, describing the flow field are transformed to associated sets of linear algebraic equations. To transfer the final form of differential equations to difference equations, the derivatives of the problem are approximated by finite centered differences. The system of algebraic equations is solved using Gauss-Siedel iteration method [22- 24]. An iterative solution procedure is employed to obtain the steady state solution of the problem considered. The grid independence test is performed using successively sized grids, 3500 × 180, 4000 × 200 and 4500 × 220 for Re = 600, A = 0.1, B = 0.5 and S=1.0. The value of average Nusselt number at sinusoidal target surface is shown in Table 1. Variations by less than 10-6 over all grid points are adopted as a convergence criterion. A uniform grid with 4000 × 200 is used in all subsequent calculations considering the same dimensionless surface wave amplitude. This procedure is repeated for all examined dimensionless surface wave amplitude. A computer program in FORTRAN is developed to perform the numerical solution of these sets. Solving the governing equations, the hydrodynamic and thermal flow fields are obtained. Consequently, local and average Nusselt numbers are derived with the aid of their definitions.

Table 1.
Comparison on average Nusselt number at several grids for Re = 600, A = 0.1, B = 0.5 and S=1.0.

Grid size	3500 × 180	4000 × 200	4500 × 200
Nu	1.8952	1.1944	1.1945

4. Results and Discussion

The proposed theoretical model is used to study the effect of Reynolds number, dimensionless slot jet width, dimensionless surface wave amplitude and dimensionless sinusoidal surface wave length on flow field and, both, local and average Nusselt number.

4.1 Validity of the present model

In order to check the validity of the model, a comparison is made between the numerical results from the present work with the corresponding experimental results reported by M. Rady et al. [25] and E. M. Sparrow et al. [26] for single slot jet as shown in Figure 2. The local Nusselt number is plotted versus dimensionless distance, X, for Reynolds number of 450 and dimensionless slot jet width, B, of 0.5 considering flat target surface (A=0.0). Good agreement is found between the present results and those obtained from previous studies.

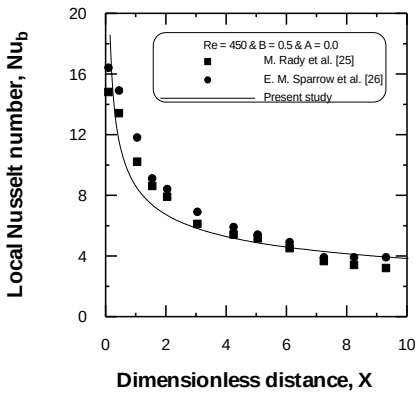

Figure 2. Comparison of the local Nusselt number between present result and those in refs. [25, 26].

4.2 The flow field

Since the spacing between jet and impinging surface is quite small, the measurement of the velocity components profiles are very difficult. The dimensionless velocity profile at Reynolds number of 400, dimensionless surface wave length, S, of 3.0 and dimensionless slot jet width, B, of 0.5 for different values of dimensionless surface wave amplitude, A, is illustrated in Figure 3.

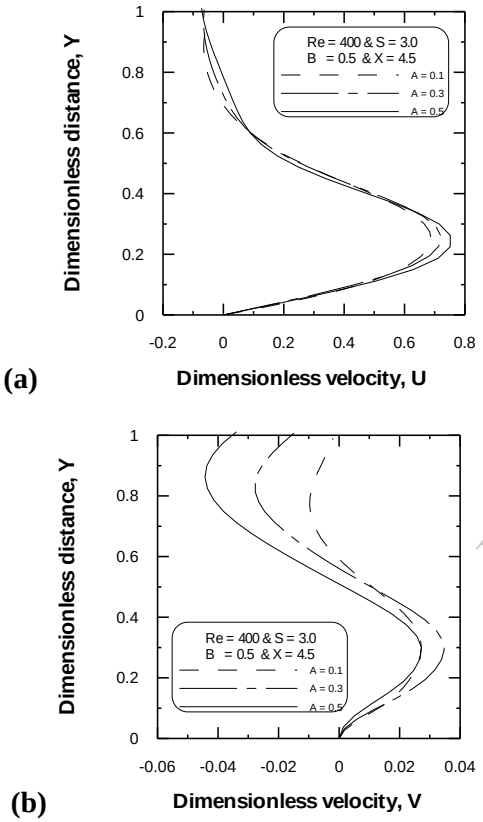

Figure 3. Dimensionless velocities profiles for different values of dimensionless sinusoidal surface amplitude at X=4.5.

This figure is presented at dimensionless axial position X = 4.5 which located at the second concave portion of sinusoidal impingement surface. Generally, the values of dimensionless velocities are increased from zero to maximum values and decreased elsewhere. The maximum values of dimensionless velocities are occurred near the adiabatic surface. At higher values of dimensionless distance, Y, negative velocities are occurred which indicated the presence of recirculation considering the concave portion of impingement surface. The value of dimensionless velocity, U, is increased with the increase of dimensionless surface wave amplitude as shown in Figure 3-a. On the other hand, the value of dimensionless velocity, V, is decreased with the increase of dimensionless surface wave amplitude as shown in Figure 3-b.

Similarly, the dimensionless velocity profile at Reynolds number of 400, dimensionless surface wave length of 3.0 and dimensionless slot jet width of 0.5 for different values of dimensionless surface wave amplitude is illustrated in Figure 4. This figure is presented at dimensionless axial position X = 9.0 which located at the third convex portion of sinusoidal impingement surface. Indeed, no negative value of dimensionless velocity, U, is noticed as shown in Figure 4-a. On the other hand, no positive value of dimensionless velocity, V, is noticed as shown in Figure 4-b. Vanish influence of sinusoidal impingement surface on fluid flow, at this section, is the suggested reason for this behaviour.

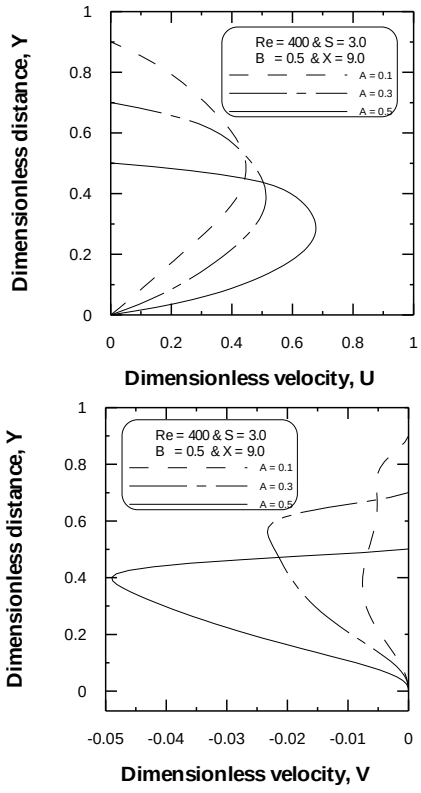

Figure 4. Dimensionless velocities profiles for different values of dimensionless sinusoidal surface amplitude at X=9.0.

4.2 Local Nusselt number

The local Nusselt number distribution, Nub, is plotted for different values of problem parameters as shown in Figure 5. and Figure 6. Maximum value of local Nusselt number is occurred at the axis of symmetry and is decreased gradually far from the jet to an asymptotic value of zero for all values of Reynolds numbers and sinusoidal surface geometries. At this point, the velocity component normal to the sinusoidal impingement surface is high and the boundary layer is additionally reduced, leading to maximum heat transfer coefficient and consequently Nusselt number. Generally, local Nusselt number distribution shows rise and fall along impingement surface. The flow reattachment with impingement surface and the recirculation zone at sinusoidal concave portions are the suggested reason for this increase.

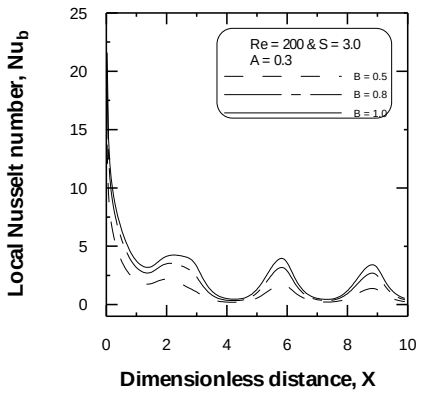

Figure 5. Local Nusselt number distribution along impingement sinusoidal surface for different values of dimensionless slot jet width at Re=200, S=3.0 and A=0.3.

The local Nusselt number distribution along impingement surface at Re = 200, dimensionless surface wave length of 3.0 and dimensionless surface wave amplitude of 0.3 for different values of dimensionless slot jet width is shown in Figure 5. The value of local Nusselt number is increased with the increase of dimensionless slot jet width. Better surface cooling, is the suggested reason for this increase. Similarly, The local Nusselt number distribution along impingement surface at Re = 200, S = 3.0 and B = 0.5 for different values of dimensionless surface wave amplitude is shown in Figure 6. The peak values of local Nusselt number are increased with the increase of dimensionless surface wave amplitude. This is expected, since the recirculation zone is increased with the increase of dimensionless surface wave amplitude.

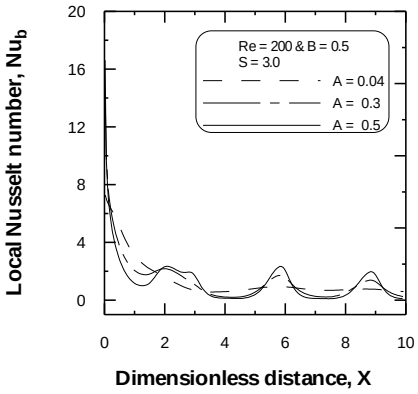

Figure 6. Local Nusselt number distribution along impingement sinusoidal surface for different values of dimensionless surface wave amplitude at Re=200, S=3.0 and B=0.5.

4.3 Average Nusselt number

Effect of dimensionless surface wave length on average Nusselt number for different values of Reynolds number and dimensionless surface wave amplitude at B=0.5 is shown in Figure 7. As expected, the values of average Nusselt number is increased with the increase of Reynolds number. Also, the values of Nu is increased with the increase of S for all values of Re with significant increase at higher values of Reynolds number and dimensionless surface wave amplitude. Better mixing due to the size increase of recirculation zones is the suggested reason for Nu increase [27-29]. Insignificant effect is found considering Nu values at values of S greater than 2.0.

Effect of dimensionless surface wave amplitude on average Nusselt number for different values of Reynolds number and dimensionless surface wave length at B=0.5 is shown in Figure 8. Also, the values of average Nusselt number is increased with the increase of Reynolds number. The values of Nu is increased with the decrease of A for all values of Re with significant changes at lower values of dimensionless surface wave length. Thus, the sinusoidal impingement surface can be an effective cooling enhancement technique at high

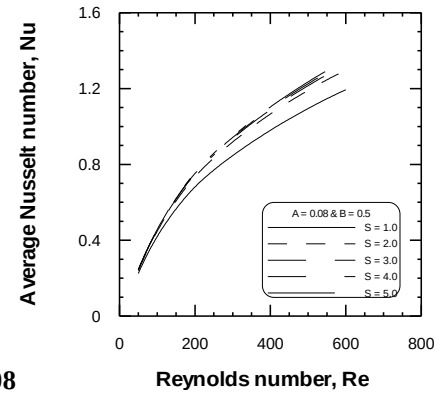

(a)A=0.08

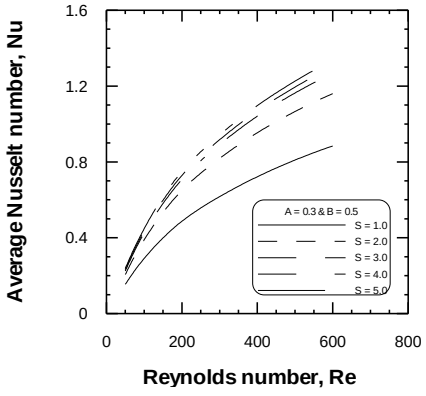

(b)A=0.3

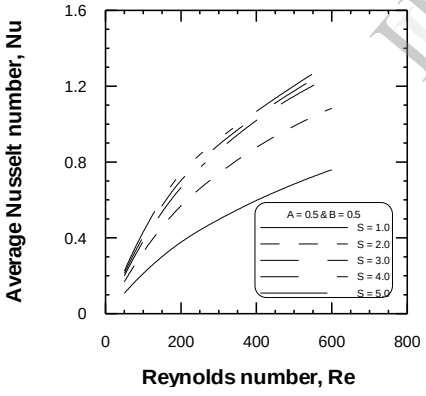

(c)A=0.5

Figure 7. Effect of dimensionless surface wave length on average Nusselt number for different values of Reynolds number at B=0.5.

Reynolds number and lower values of dimensionless surface wave amplitude.

Effect of dimensionless slot jet width on average Nusselt number for different values of dimensionless surface wave length at A=0.3 is shown in Figure 9. Generally, the values of Nu is increased with the increase of B for all values of Re while, all curves have the same trend. The values of Nu is increased with the increase of S and Reynolds number with significant increase at higher values of Re.

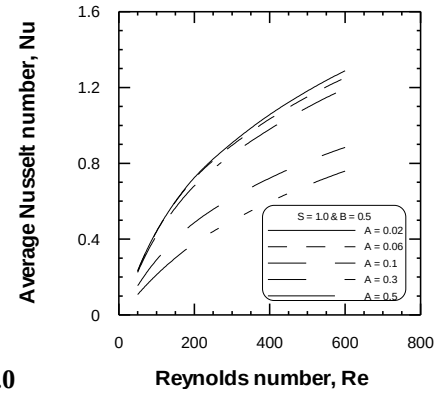

(a) S=1.0

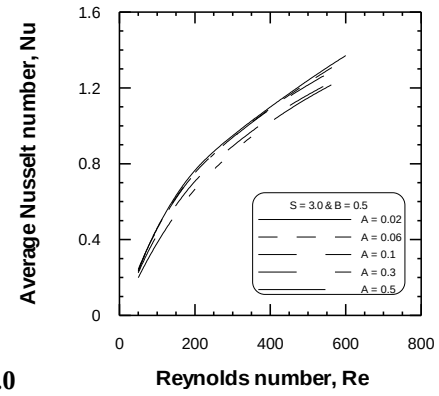

(b) S=3.0

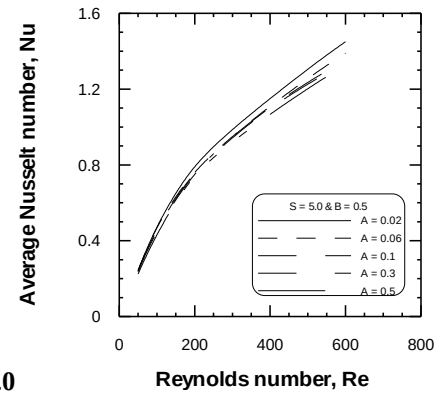

(c) S=5.0

Figure 8. Effect of dimensionless surface wave amplitude on average Nusselt number for different values of Reynolds number at B=0.5.

5. Conclusions

In the present work, the laminar flow field and heat transfer characteristics of a slot jet impinging onto a sinusoidal target surface is investigated numerically. Air is used as working fluid with constant properties taking into consideration uniform jet velocity exit impinging on a sinusoidal target surface of uniform temperature. The effect of problem parameters: Reynolds number (Re = 50 - 600), dimensionless slot jet width (B = 0.5 – 1.0), dimensionless surface wave amplitude (A = 0.0 - 0.5) and dimensionless surface wave length (S = 1.0 – 5.0) is presented.

The flow field, local Nusselt number and, in turn, average Nusselt at the impinging wall are evaluated at different values of the problem parameters. The sinusoidal target surface induces lateral vortices in the concave regions, which grow in magnitude and spatial flow coverage depending on problem parameters. The average Nusselt number is increased with the increase of jet Reynolds number, dimensionless surface wave length and dimensionless slot jet width. On the other hand, it is decreased with the increase of dimensionless surface wave amplitude. While, insignificant effect is found considering Nu values at values of dimensionless surface wave length greater than 2.0. Maximum value of local Nusselt number is occurred at the axis of symmetry and is decreased gradually far from the jet to an asymptotic value of zero. The peak values of local Nusselt number are increased with the increase of dimensionless surface wave amplitude. Increasing the dimensionless surface wave amplitude has the most significant effect on heat transfer enhancement. This may be attributed to enlargement of the recirculation flow zones. The sinusoidal impingement surface can be an effective cooling enhancement technique at high Reynolds number and lower values of dimensionless surface wave amplitude and dimensionless surface wave length.

(a)Re=50

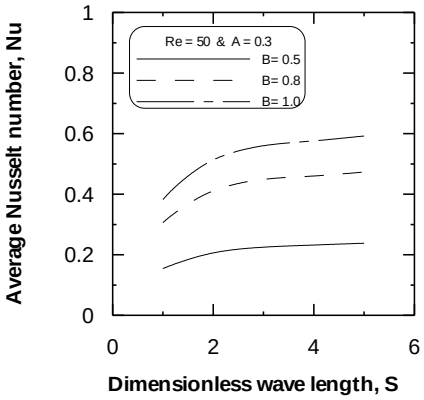

(b)Re=200

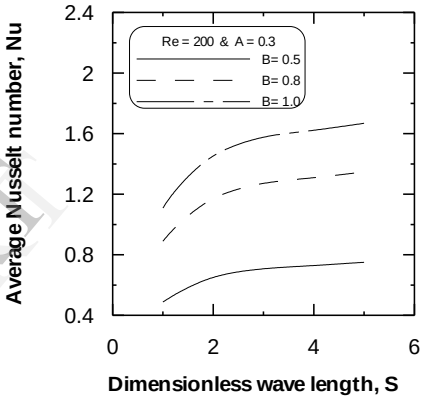

(c)Re=600

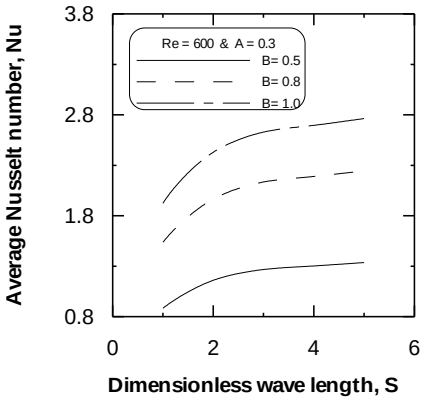

Figure 9. Effect of dimensionless slot jet width on average Nusselt number for different values of surface wave length at A=0.3.

References

[1] R. Gardon, and J.C. Akfirat, "Heat transfer characteristics of impinging two-dimensional air jets", ASME Journal of Heat Transfer 88 (1966), pp. 101–108.
[2] S.J. Downs, and E.H. James, "Jet impingement heat transfer – a literature survey", ASME paper 87-HT-35, ASME, New York, 1987.
[3] S.V. Garimella, "Heat transfer and flow fields in confined jet impingement", Annual Rev Heat Transfer, 11 (2000), pp. 413–494.
[4] H. Chattopadhyay, and S.K. Saha, "Turbulent heat transfer from a slot jet impinging on a moving plate", International Journal of Heat and Fluid Flow, 24 (2003), pp. 685–697.
[5] M.K. Isman, E. Pulat, and A. B. Etemoglu, M. Can," Numerical analysis of flow and heat transfer characteristics of impinging slot air jets", Journal of Thermal Science and Technology, 25 (2005), pp. 17–24.
[6] H.G. Lee, H.S. Yoon, and M.Y. Ha, "A numerical investigation on the fluid flow and heat transfer in the confined impinging slot jet in the low Reynolds number region for different channel heights", International Journal of Heat and Mass Transfer, 51 (2008), pp. 4055–4068.
[7] I. Dagtekin, and H.F. Oztop, "Heat transfer due to double laminar slot jets impingement onto an isothermal wall within one side closed long duct", International Communications in Heat and Mass Transfer, 35 (2008), pp. 65–75.
[8] M.A.R. Sharif, and A. Banerjee, "Numerical analysis of heat transfer due to confined slot-jet impingement on a moving plate", Applied Thermal Engineering, 29 (2009), pp. 532–540.
[9] K. Ibuki, T. Umeda, H. Fujimoto, H. Takuda, "Heat transfer characteristics of a planar water jet impinging normally or obliquely on a flat surface at relatively low Reynolds numbers", Experimental Thermal and Fluid Science, 33 (2009), pp. 1226–1234.
[10] K.S. Choo, and S.J. Kim, "Comparison of thermal characteristics of confined and unconfined impinging jets", International Journal of Heat and Mass Transfer, 53 (2010), pp. 3366–3371.
[11] K. Na-pompet, and W. Boonsupthip, "Effect of a narrow channel on heat transfer enhancement of a slot-jet impingement system", Journal of Food Engineering, 103 (2011), pp. 366–276.
[12] C.S. McDaniel, and B.W. Webb, "Slot jet impingement heat transfer from circular cylinders", International Journal of Heat and Mass Transfer, 43 (2000), pp. 1975–1985.
[13] T.L. Chan, Y. Zhou, M.H. Liu, and C.W. Leung, "Mean flow and turbulence measurements of the impingement wall jet on a semi-circular convex surface", Experimental Fluids, 34 (2003), pp. 140–149.
[14] F. Gori, and L. Bossi, "Optimal slot height in the jet cooling of a circular cylinder", Applied Thermal Engineering, 23 (2003), pp. 859–870.
[15] K. Kanokjaruvijit, and R.F. Martinez-Botas, "Jet impingement on a dimpled surface with different cross flow schemes", International Journal of Heat and Mass Transfer, 48 (2005), pp. 16–170.
[16] S.Z. Shuja, B. Yilbas, S. Ma, and S. Khan, "Jet emerging from an annular nozzle and impinging onto cylindrical cavity: effect of jet velocity on flow structure and heat transfer rates", Proceeding I Mechanical Engineering Part C., Journal of Mechanical Engineering Science, 222 (2008), pp. 1021–1031.
[17] V.I. Terekhov, S.V. Kalinina, Yu.M. Mshvidobadze, and K.A. Sharov, "Impingement of an impact jet onto a spherical cavity", Flow structure and heat transfer, International Journal of Heat and Mass Transfer, 52 (2009), pp. 2498–2506.
[18] M.A.R. Sharif, and K.K. Mothe, "Parametric study of turbulent slot-jet impingement heat transfer from concave cylindrical surfaces", International Journal of Thermal Science, 49 (2010), pp. 428–442.
[19] N. Celik, "Effects of the surface roughness on heat transfer of perpendicularly impinging co-axial jet", Heat Mass Transfer, 47 (2011), pp. 1209–1217.
[20] Y.T. Yang, T.C. Wei, and Y.H. Wang, "Numerical study of turbulent slot jet impingement cooling on a semi-circular concave surface", International Journal of Heat and Mass Transfer, 54 (2011), pp. 482–489.
[21] Y. Varol, D.E. Alnak, H.F. Oztop, and K. Al-Salem, "Numerical analysis of heat transfer due to slot jets impingement onto two cylinders", International Communications in Heat and Mass Transfer, 39 (2012), pp. 726–735.
[22] S.V. Patankar, "Numerical Heat Transfer and Fluid Flow", Hemisphere Publishing Co., New York, (1980), pp. 113–147.
[23] M.N. Ö zisik, "Finite Difference Methods in Heat Transfer," CRC Press, London, (1994), pp. 307–353.
[24] J.F. Thompson, Z.U.A. Warsi, and C.W. Mastin, "Numerical Grid Generation", North Holland, (1985), pp. 188–235.
[25] M. Rady and E. Arquis, "Heat transfer enhancement of multiple impinging slot jets with symmetric exhaust ports and confinement surface protrusions", Applied Thermal Engineering, 26 (2006), pp. 1310–1319.
[26] E.M. Sparrow and T.S. Wong, "Impingement transfer due to initially laminar slot jets", International Journal Heat Mass Transfer, 18 (1975), pp. 597–605.
[27] G. Wang and S.P. Vanka, "EHD Enhanced Heat Transfer in Wavy Channel", Int. Comm. Heat Mass Transfer, Vol.32 (2005), pp. 809–821.
[28] Q.W. Wang, G.N. Xie, M. Zing and L.Q. Luo, "Numerical investigation of heat transfer and fluid flow inside a wavy channel", Heat and Mass transfer 42 (2006), pp. 243–252.
[29] S. Vyas, J. Zhang and R. Manglik, "Steady Recirculation and Laminar Forced Convection in a Sinusoidal Wavy Channel", ASME Journal of Heat Transfer, 126 (2007), pp. 500–510.

Nomenclature

a	Sinusoidal surface wave amplitude	m
A	Dimensionless surface wave amplitude	--
b	Width of slot jet	m
B	Dimensionless slot jet width	--
H	Spacing between jet and impinging surface	m

h	Heat transfer coefficient	W/m^2 K
k	Thermal conductivity of fluid	W/m K
l	Length computational domain	m
L	Dimensionless length computational domain	
Nu_b	Local Nusselt number (h b/k)	--
Nu	Average Nusselt number	--
P	Pressure	N/m^2
Pr	Prandtl number (ν/α)	--
s	Sinusoidal surface wave length	m
S	Dimensionless surface wave length	--
T	Temperature	K
Re	Reynolds number (v_i b/ν)	--
u, v	Velocity components in x and y directions	m/s
U, V	Dimensionless velocity	--
x, y	Cartesian coordinates	m
X, Y	Dimensionless coordinates	--
Greek symbols		
α	Thermal diffusivity	m^2/s
ρ	Density	kg/m^3
ν	Kinematics viscosity	m^2/s
θ	Dimensionless temperature	--
Subscripts		
∞	Ambient	
e	Test section exit	
j	Jet exit	
s	Sinusoidal surface	